

Structures and Sorption Properties of 2-Methylbenzimidazolate-Based Zn(II) Frameworks

Won Ju Phang, Woo Ram Lee, and Chang Seop Hong*

Department of Chemistry, Research Institute for Natural Sciences, Korea University, Seoul 136-713, Korea

*E-mail: cshong@korea.ac.kr

Received March 6, 2014, Accepted April 23, 2014

The syntheses and crystal structures of a three-dimensional (3D) coordination network $[\text{Zn}_4(2\text{-mBIM})_5(\text{C}_2\text{H}_6\text{NCOO})(\text{HCOO})(\mu\text{-OH})]\cdot\text{DMF}$ (**1**·DMF; 2-mBIM = 2-methylbenzimidazolate) and a two-dimensional (2D) layer $[\text{Zn}_2(2\text{-mBIM})_3(\text{HCOO})(\text{H}_2\text{O})]\cdot\text{DMF}$ (**2**·DMF) are reported. Different structures were produced depending on the ratio of reactants. Structurally, **1** illustrates the formation of a unique framework based on a 2-mBIM bridge with the side group on an imidazole ring, while **2** possesses a honeycomb layer built up purely from imidazoles. For gas sorption, CO_2 is adsorbed on the activated phase of **1** but N_2 is not taken up.

Key Words : Metal-organic frameworks, Imidazolate, Sorption

Introduction

Much interest has been devoted to the research of metal-organic frameworks (MOFs), as they are porous crystalline materials with high surface areas and adjustable pore sizes. Such porous solids have potential applications in various fields such as in gas storage, separation, and catalysis.¹⁻⁴ However, many MOFs suffer from chemical and thermal instabilities and thus their use is limited. As a new class of MOFs, zeolitic imidazolate frameworks (ZIFs) have emerged as potential improvements over conventional MOFs, and the bridging angle ($\sim 145^\circ$) of M-imidazolate-M coincides with the Si-O-Si angle that is preferably found in conventional zeolites. These frameworks exert better structural stability owing to the stronger metal-imidazolate interaction.⁵

Benzimidazolate (BIM) is utilized in the construction of many ZIFs in which a variant is exclusively located on the side group of the benzene ring of BIM.^{6,7} In comparison, 2-methylbenzimidazolate (2-mBIM) with a methyl group on the imidazole ring has been demonstrated as cations in salts, bridging ligands in metallacalix[4]arenes, and monodentate capping ligands in mononuclear complexes.⁸⁻¹³ However, multi-dimensional frameworks based on 2-mBIM to mimic the binding modes of ZIFs are still scarce in the literature.^{6,7}

Herein we report the syntheses and crystal structures of a three-dimensional (3D) framework $[\text{Zn}_4(2\text{-mBIM})_5(\text{C}_2\text{H}_6\text{NCOO})(\text{HCOO})(\mu\text{-OH})]\cdot\text{DMF}$ (**1**·DMF) and a two-dimensional (2D) sheet $[\text{Zn}_2(2\text{-mBIM})_3(\text{HCOO})(\text{H}_2\text{O})]\cdot\text{DMF}$ (**2**·DMF). The 3D framework with 2-mBIM demonstrates a singular example among benzimidazolate-based ZIFs. Meanwhile, a unique honeycomb layer is formed in **2** via 2-mBIM bridging pathways. For **1**, CO_2 sorption occurs whereas N_2 is not adsorbed.

Experimental

$[\text{Zn}_4(2\text{-mBIM})_5(\text{C}_2\text{H}_6\text{NCOO})(\text{HCOO})(\mu\text{-OH})]\cdot\text{DMF}$

(**1**·DMF). A solution of $\text{ZnBr}_2\cdot\text{H}_2\text{O}$ (0.41 g, 1.82 mmol) in 5 mL of water was slowly added to a solution of 2-mBIMH (0.72 g, 5.45 mmol) in 15 mL of DMF with stirring. The reaction mixture was additionally stirred at room temperature for 1 h. Portions of the resulting solution (4 mL) was transferred to individual 10 mL vials, after which the vials were sealed and heated at 100°C for 8 d. The resulting colorless cubic crystals were filtered and washed with DMF and dried in the air. The final yield was calculated to be 68%. Anal. Calcd for $\text{C}_{47}\text{H}_{50}\text{N}_{12}\text{O}_6\text{Zn}_4$: N, 14.75; C, 49.54; H, 4.33. Found: N, 14.87; C, 49.29; H, 4.68.

$[\text{Zn}_2(2\text{-mBIM})_3(\text{HCOO})(\text{H}_2\text{O})]\cdot\text{DMF}$ (**2**·DMF). A solution of 2-mBIMH (1.20 g, 9.10 mmol) in DMF (15 mL) was added to a solution of $\text{ZnBr}_2\cdot\text{H}_2\text{O}$ (0.41 g, 1.82 mmol) in water (5 mL) and the resulting mixture was stirred for 1 h. A 4 mL portion of the resulting solution was placed in individual vials. After sealing, the vials were placed in an oven and heated at 100°C for 8 d. The colorless plate crystals were collected by filtration, washed with DMF, and dried in air. The final yield was 75%. Anal. Calcd for $\text{C}_{28}\text{H}_{29}\text{N}_7\text{O}_4\text{Zn}_2$: N, 14.85; C, 50.93; H, 4.73. Found: N, 14.99; C, 50.96; H, 4.65.

Physical Measurements. Elemental analysis for C, H, and N was performed at the Elemental Analysis Service Center of Sogang University. Thermogravimetric (TG) analyses were carried out at a ramp rate of $10^\circ\text{C}/\text{min}$ under a N_2 flow (50 mL/min) using a Scinco TGA N-1000 instrument. Powder X-ray diffractograms were recorded using $\text{Cu K}\alpha$ ($\lambda = 1.5406 \text{ \AA}$) on a Rigaku Ultima III diffractometer with a scan speed of $2^\circ/\text{min}$ and a step size of 0.02° .

Gas Sorption Measurements. Gas sorption isotherms were measured using a BEL Belsorp mini II gas adsorption instrument with up to 1 atm of gas pressure. Highly pure N_2 (99.999%) and CO_2 (99.999%) were used in the sorption experiments. The gases isotherms were measured at 77 K (N_2), 195 K (CO_2), 273 K (CO_2), and 298 K (CO_2).

Crystallographic Structure Determination. X-ray data

for **1** and **2** were collected on a Bruker SMART APEXII diffractometer equipped with graphite monochromated Mo K α radiation ($\lambda = 0.71073 \text{ \AA}$). The preliminary orientation matrix and cell parameters were determined from three sets of ϕ scans at different starting angles. Data frames were obtained at scan intervals of 0.5° with an exposure time of 20 s per frame. The reflection data were corrected for Lorentz and polarization factors. Absorption corrections were carried out using the program SADABS. The structures of **1** and **2** were solved by direct methods and refined by full-matrix least-squares analysis using anisotropic thermal parameters for non-hydrogen atoms with the SHELXTL program. Crystal data of **1**: empirical formula = $C_{47}H_{49}N_{12}O_6Zn_4$, Mr = 1139.46, monoclinic, space group $P2_1/c$, $a = 18.2794(3) \text{ \AA}$, $b = 15.8441(3) \text{ \AA}$, $c = 19.8023(4) \text{ \AA}$, $\beta = 119.014(1)^\circ$, $V = 5015.40(16) \text{ \AA}^3$, $Z = 4$, $D_{\text{calc}} = 1.509 \text{ g cm}^{-3}$, $\mu = 1.949 \text{ mm}^{-1}$, 12450 reflections collected, 6748 unique ($R_{\text{int}} = 0.1150$), $R1 = 0.0783$, $wR2 = 0.1586 [I > 2\sigma(I)]$. Crystal data of **2**: empirical formula = $C_{28}H_{29}N_7O_4Zn_2$, Mr = 658.32, triclinic, space group $P-1$, $a = 10.309(5) \text{ \AA}$, $b = 10.341(4) \text{ \AA}$, $c = 16.602(8) \text{ \AA}$, $\alpha = 10.309(5)^\circ$, $\beta = 72.57(3)^\circ$, $\gamma = 61.85(2)^\circ$, $V = 1479.9(11) \text{ \AA}^3$, $Z = 2$, $D_{\text{calc}} = 1.477 \text{ g cm}^{-3}$, $\mu = 1.666 \text{ mm}^{-1}$, 7231 reflections collected, 4213 unique ($R_{\text{int}} = 0.0898$), $R1 = 0.0578$, $wR2 = 0.2053 [I > 2\sigma(I)]$. Crystallographic data for the structures reported here have been deposited with CCDC (Deposition No. CCDC-989462 (**1**) and 989463 (**2**)). These data can be obtained free of charge via <http://www.ccdc.cam.ac.uk/conts/retrieving.html> or from CCDC, 12 Union Road, Cambridge CB2 1EZ, UK, E-mail: deposit@ccdc.cam.ac.uk.

Results and Discussion

Synthesis and Structures. A solvothermal reaction of Zn^{2+} and 2-mMBIH in DMF/H $_2$ O was conducted with different ratios of reactants. When the ratio of Zn^{2+} and 2-mBIMH was 1:3, complex **1** with a 3D structure was formed, while a ratio of 1:5 resulted in a 2D layered sheet compound (**2**). Although the reaction temperature, solvent, and time were the same, the ratio of the reactants allowed for the generation of entirely different structures. The elemental analysis showed that the ratio of Zn and 2-mBIM in the chemical formula of **1** was greater than that of **2**, which reflected the reaction conditions.

In the crystal structure of **1** (Figure 1), four crystallographically different Zn sites are present. The Zn1 and Zn2 atoms are tetrahedrally surrounded by two N atoms from two 2-mBIM ligands and two O atoms from OH $^-$ and dimethylcarbamate bridges, while the other Zn atoms (Zn3 and Zn4) are coordinated by three N atoms from three 2-mBIM ligands and one O atom from the formate bridge. A simple geometry index for four-coordinate systems was proposed by Houser and coworkers¹⁴ and the formula is given by $\tau_4 = [360 - (\alpha + \beta)]/141$ where α and β are the two largest angles. The indices obtained in the current work are in the range of 0.93 – 0.96 for the Zn coordination spheres, indicating that their geometry belongs to a distorted tetra-

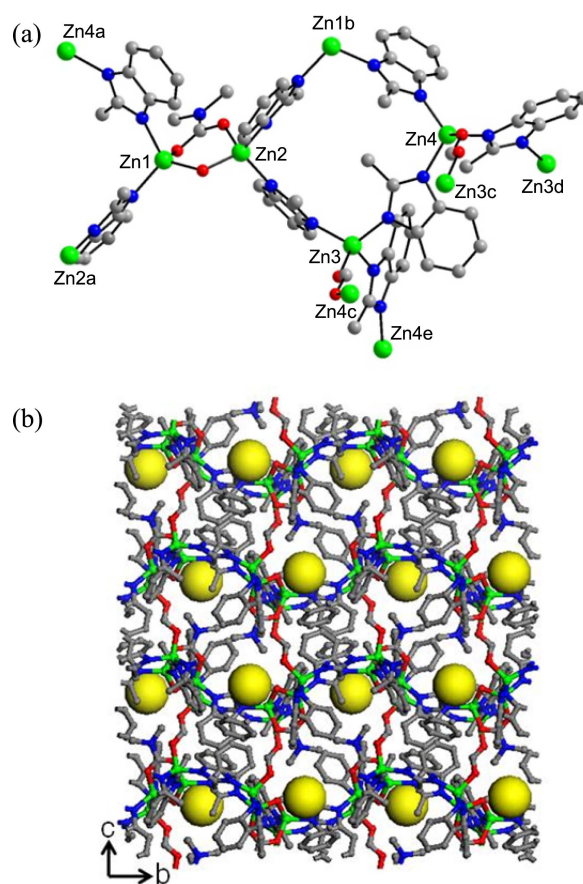


Figure 1. (a) Molecular structure of **1** showing coordination environments. Symmetry code: a = $3-x, -0.5+y, 1.5-z$; b = $3-x, 0.5+y, 1.5-z$; c = $4-x, 2-y, 2-z$; d = $4-x, 0.5+y, 1.5-z$; e = $4-x, -0.5+y, 1.5-z$. (b) Extended 3D view containing voids.

hedron. The *in-situ* formation of dimethyl carbamate, formate, and hydroxide has been reported in the literature under solvothermal reactions.¹⁵⁻²¹ The dimethyl carbamate¹⁹⁻²¹ and formate¹⁶⁻¹⁸ ligands were suggested to be generated from the decomposition pathways of DMF molecules under vigorous conditions. The dimethyl carbamate and formate ligands connect Zn1 and Zn2 in the *syn-syn* mode of carbamate oxygens, and Zn3 and Zn4 in the *anti-anti* mode of formate oxygens, respectively. An interesting observation is that the hydroxide¹⁵ molecule participates in bridging adjacent Zn centers together with the carbamate group. The 2-mBIM moiety serves as another bridging group to link all Zn atoms, eventually leading to the formation of a three-dimensional framework with the support of the other bridges.

To assay the network topology, the double bridges and single linkers are designated by sticks and the Zn atoms are placed at the joints. This framework is a 2-nodal net with 3,4-centered net with stoichiometry (3-c)(4-c) and a point symbol is $\{4.8^2\}\{4^2.6.8^3\}$. The topological type belongs to **cbs/CrB** self-dual system.²² The 3D structure contains DMF molecules in the lattice. The yellow spheres denote the positions of DMF molecules to provide void spaces in the framework. The solvent-accessible void volume was calculated by the program PLATON to be 17%.

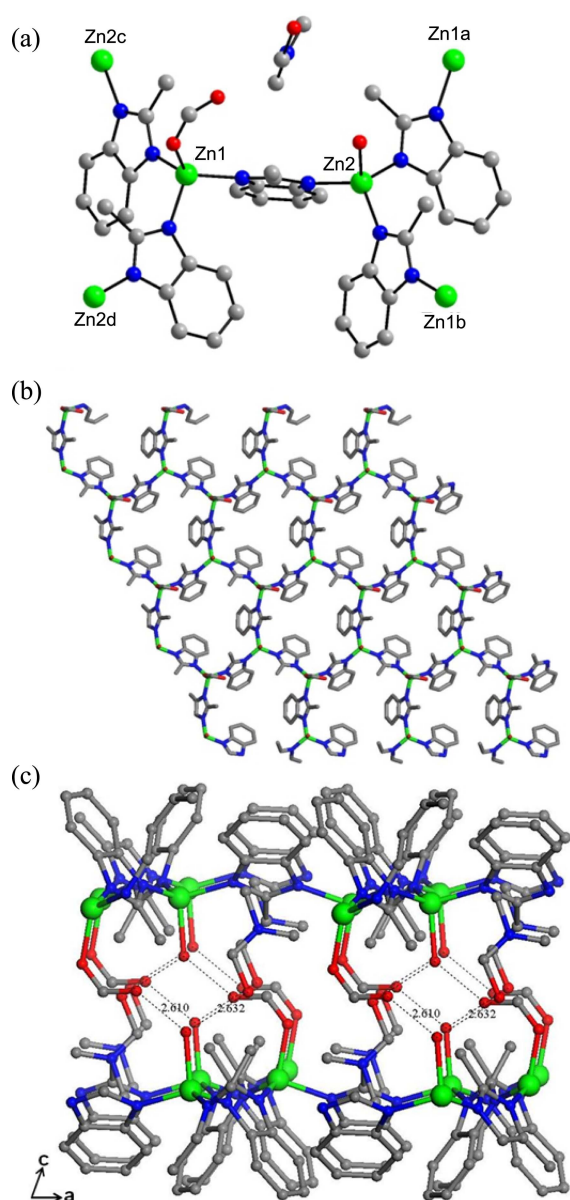


Figure 2. (a) Molecular structure of **2** showing coordination environments. Symmetry code: $a = -1+x, y, z$; $b = -1+x, 1+y, z$; $c = 1+x, -1+y, z$; $d = 1+x, y, z$. (b) 2D layered structure. (c) Extended view representing H bonds in the ac plane.

The crystal structure of **2** shows that two different Zn sites (Zn1 and Zn2) are present in the asymmetric unit (Figure 2). The Zn1 center is coordinated by three N atoms from three 2-mBIM bridges and one O atom from the terminal formate ligand. The τ_4 values for the central atoms are 0.93 for Zn1 and 0.92 for Zn2, which are consistent with a distorted tetrahedral geometry. The two Zn atoms are bridged by 2-mBIM to generate a 2D honeycomb sheet. Evaluation of topology analysis on **2** indicates that the structure consists of layers (0 0 1) with Zn. The 2D lattice is a 3-connected hexagonal plane net with a point symbol of $\{6^3\}$ and a topological type of **hcb**. For the specific interaction, the coordinated water molecule is hydrogen-bonded to the lattice DMF molecule with an O...O distance of 2.632 Å

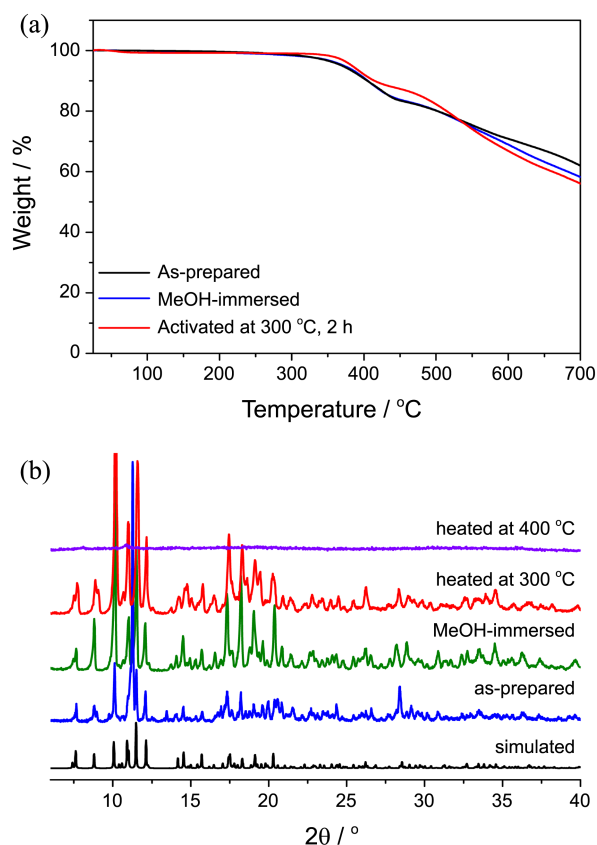


Figure 3. (a) TG curves of as-prepared (**1**·DMF), MeOH-exchanged, and activated samples. (b) PXRD profiles of simulated, as-prepared, MeOH-immersed, and samples heated at 300 and 400 °C for 2 h.

and additionally to the formate oxygen atom with an O...O distance of 2.610 Å. As a result, the single layer enables interactions with an adjacent layer through hydrogen bonding, leading to the formation of a paired double layer (Figure 2(c)). The double layers are stacked in the crystal packing diagram.

Gas Sorption Properties. TG analysis on the as-prepared sample of **1** shows that the weight of the framework begins to be lost at ~300 °C, which is attributed to the simultaneous decomposition of coordinate components and DMF molecules in the lattice. Sample **1** was then soaked in MeOH for 3 d and TG data were subsequently collected for the MeOH-immersed sample. The thermal decomposition profile of this sample is similar to that of the as-prepared one, suggesting that the solvent exchange is not effective for this system. Powder X-ray diffraction (PXRD) profiles were recorded to identify the phase of the solids. The profiles of the as-prepared sample (**1**·DMF) are consistent with that of the simulated one, supporting the phase purity of the bulk sample. The PXRD pattern of the MeOH-immersed solid agrees well with that of the as-prepared sample, reflecting that the structure is maintained during the MeOH soaking treatment. The sample was heated in vacuum at 300 °C for 2 h to produce the activated phase. The activated framework remains intact, as confirmed by the PXRD data. The DMF

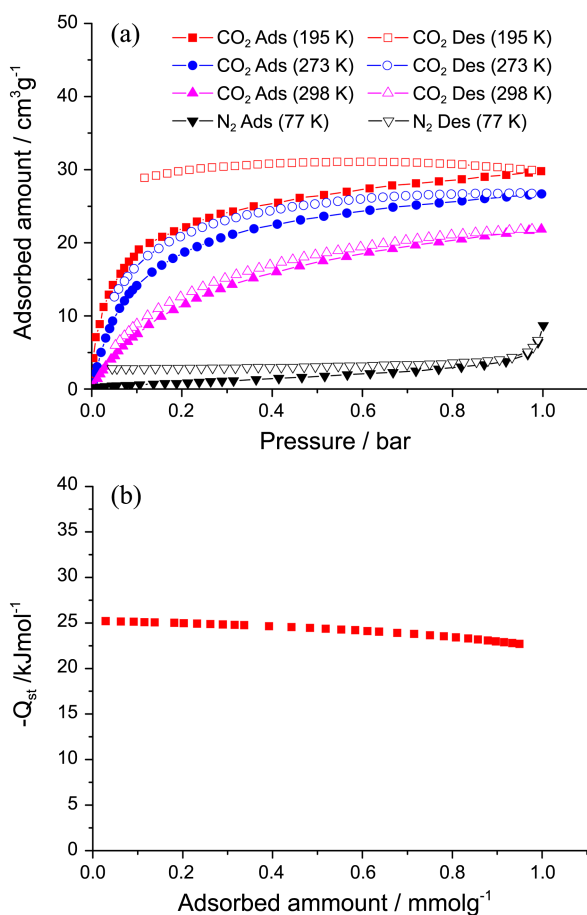


Figure 4. (a) Gas sorption isotherms of **1**. (b) Isosteric heat of CO₂ adsorption of **1**.

molecules appears to be partially removed from the lattice upon the activation process as the weight loss in the TG curve of the activated phase at approximately 300 °C is smaller than that of the as-prepared one. When an elevated temperature of 400 °C was applied for 2 h in an attempt to eliminate all of the DMF molecules, the framework was observed to completely collapse (Figure 3(b)). The phase purity of **2** was also ascertained by PXRD.

The N₂ sorption isotherms at 77 K for the activated sample of **1** show negligible adsorption (Figure 4(a)), while CO₂ is adsorbed on the sample; thus, typical type I behavior is observed. The observed sorption behavior may be associated with the different kinetic diameters of both gases. The Brunauer–Emmett–Teller surface area was calculated from the CO₂ sorption data at 195 K to be 103 m²/g. From the isotherm data for CO₂ at 273 and 298 K, the isosteric heat of adsorption (-Q_{st}) was determined on the basis of a virial-type equation. The obtained adsorption enthalpy is 22.7–25.2 kJ/mol, which corresponds to the usual values observed for carboxylate-linked MOFs (Figure 4(b)).¹

Conclusion

We have prepared imidazolate-bridged Zn(II) coordina-

tion frameworks with a 3D network (**1**) and 2D layered structure (**2**). The different structures were produced when the ratios of reactants were changed. The 3D architecture, constructed from 2-mBIM, is a unique example since ZIFs composed of benzimidazolate (BIM) typically have side groups on the benzene ring, and not on the imidazole ring. An interesting honeycomb sheet is observed in complex **2**, and this is produced as a consequence of 2-mBIM linkage throughout the 2D lattice. The activated phase of **1** shows CO₂ adsorption while N₂ is not adsorbed on the sample.

Acknowledgments. This work was supported by the Korea CCS R&D Center (KCRC) grant funded by the Korea government (The Ministry of Science, ICT & Future Planning (MSIP)) (NRF-2013M1A8A1035849), by Basic Science Research Program (NRF-2012R1A1A2007141), and by the Priority Research Centers Program (NRF20100020209).

References

- Sumida, K.; Rogow, D. L.; Mason, J. A.; McDonald, T. M.; Bloch, E. D.; Herm, Z. R.; Bae, T. H.; Long, J. R. *Chem. Rev.* **2012**, *112*, 724.
- Suh, M. P.; Park, H. J.; Prasad, T. K.; Lim, D. W. *Chem. Rev.* **2012**, *112*, 782.
- Li, J. R.; Sculley, J.; Zhou, H. C. *Chem. Rev.* **2012**, *112*, 869.
- Yoon, M.; Srirambalaji, R.; Kim, K. *Chem. Rev.* **2012**, *112*, 1196.
- Park, K. S.; Ni, Z.; Cote, A. P.; Choi, J. Y.; Huang, R.; Uribe-Romo, F. J.; Chae, H. K.; O'Keeffe, M.; Yaghi, O. M. *Proc. Natl. Acad. Sci. USA* **2006**, *103*, 10186.
- Banerjee, R.; Phan, A.; Wang, B.; Knobler, C.; Furukawa, H.; O'Keeffe, M.; Yaghi, O. M. *Science* **2008**, *319*, 939.
- Banerjee, R.; Furukawa, H.; Britt, D.; Knobler, C.; O'Keeffe, M.; Yaghi, O. M. *J. Am. Chem. Soc.* **2009**, *131*, 3875.
- Cameron, T. S.; Clyburne, J. A. C.; Dubey, P. K.; Grossert, J. S.; Ramaiah, K.; Ramanatham, J.; Sereida, S. V. *Can. J. Chem.* **2003**, *81*, 612.
- Rufino-Felipe, E.; Munoz-Hernandez, M. A. *Chem. Commun.* **2011**, 3210.
- Rufino-Felipe, E.; Munoz-Hernandez, M. A.; Saucedo-Azpeitia, H. F.; Cortes-Llamas, S. A. *Inorg. Chem.* **2012**, *51*, 12834.
- Bhattacharya, R.; Chanda, S.; Bocelli, G.; Cantoni, A.; Ghosh, A. *J. Chem. Crystallogr.* **2004**, *34*, 393.
- Sanchez-Guadarrama, O.; Lopez-Sandoval, H.; Sanchez-Bartez, F.; Gracia-Mora, I.; Hopfl, H.; Barba-Behrens, N. *J. Inorg. Biochem.* **2009**, *103*, 1204.
- Tarte, N. H.; Woo, S. I.; Cui, L.; Gong, Y.-D.; Hwang, Y. H. *J. Organomet. Chem.* **2008**, *693*, 729.
- Yang, L.; Powell, D. R.; Houser, R. P. *Dalton Trans.* **2007**, 955.
- Jeon, H. R.; Min, D. W.; Oh, Y.; Lee, E.; Kim, Y.; Jung, D. Y.; Kim, J. *Bull. Korean Chem. Soc.* **2008**, *29*, 2540.
- Dai, F.; Cui, P.; Ye, F.; Sun, D. *Cryst. Growth Des.* **2010**, *10*, 1474.
- Guo, J.; Sun, D.; Zhang, L.; Yang, Q.; Zhao, X.; Sun, D. *Cryst. Growth Des.* **2012**, 5649.
- Huh, H. S.; Lee, S. W. *Bull. Korean Chem. Soc.* **2008**, *29*, 2383.
- An, J.; Fiorella, R. P.; Geib, S. J.; Rosi, N. L. *J. Am. Chem. Soc.* **2009**, *313*, 8401.
- Dell'Amico, D. B.; Calderazzo, F.; Labella, L.; Marchetti, F. *Inorg. Chim. Acta* **2003**, *350*, 661.
- McCowan, C. S.; Groy, T. L.; Caudle, M. T. *Inorg. Chem.* **2002**, *41*, 1120.
- Blatov, V. A.; Shevchenko, A. P. *TOPOS (Ver. 4.0) Samara State University, Russia*. 2011.